Lateral photovoltaic effects in $Bi_2Sr_2Co_2O_y$ thin films

Guoying Yan (闫国英)[1,2], Guangsheng Fu (傅广生)[1,2*], Zilong Bai (白子龙)[2], and Shufang Wang (王淑芳)[2]

[1] *School of Information Engineering, Hebei University of Technology, Tianjin 300401, China*

[2] *The College of Physics Science and Technology, Hebei University, Baoding 071002, China*

[*] *Corresponding author: m_ygy@126.com*

Received August 26, 2013; accepted October 17, 2013; posted online December 5, 2013

Lateral photovoltaic (LPV) effects are observed in $Bi_2Sr_2Co_2O_y$ (BSCO) thin films. Upon illumination of a 532-nm constant laser, the lateral photovoltage is observed to vary linearly with the laser position between two electrodes on the film surface, and the position sensitivity can be enhanced by coating a layer of graphite on the surface of the BSCO film as a light absorber. Results suggest that the LPV effect in the thin film is independent of the photo-generated carriers but originates from thermoelectric effects. The present work demonstrates a potential application of BSCO films in position-sensitive photo (thermal) detectors.

OCIS codes: 310.6845, 040.5160, 240.0310.

doi: 10.3788/COL201311.123101.

Transition metal oxides form an attractive class of materials because of their potential applications in thermoelectric or optoelectronic devices[1−4]. $Bi_2Sr_2Co_2O_y$ (BSCO), a newly discovered strongly correlated transition metal oxide and one of the most attractive members of this class, has attracted great attention as a promising p-type thermoelectric material because of its excellent thermoelectric performance and chemical stability in air[5−7]. Aside from its thermoelectric activity, BSCO has many other remarkable properties, including anisotropic electrical and magnetic properties, low-temperature negative magnetoresistance effects, photoelectric effects, and so on[8,9]. In this letter, we report the presence of lateral photovoltaic (LPV) effects in BSCO films to expand the application potential of the material in position-sensitive photo (thermal) detectors.

A BSCO thin film with a thickness of about 150 nm is grown on a $LaAlO_3$ (001) single crystal substrate using the chemical solution deposition method. Details of the film fabrication and structural characterization process are described in Ref. [10]. The surface morphology of the film is analyzed by an XL30 S-FEG field-emission scanning electron microscope (FE-SEM). During LPV effect measurement, two In electrodes with a diameter of 0.5 mm are placed on the film surface. A 532-nm continuous wavelength laser with a spot diameter of 1.5 mm is used as the light source, and laser-induced lateral photovoltages are recorded using a 2700 Keithley source meter.

The top inset in Fig. 1 shows a SEM image of the surface of the BSCO film. A very smooth and dense surface is observed, and the nearly uniform morphology is favorable for obtaining LPV signals with good linearity[11]. A schematic illustration of the LPV measurements is shown in the bottom inset in the same figure; here, the distance between the two In electrodes A and B is 9 mm, and the power of the illuminating laser is fixed at 20 mW. Figure 1 displays the lateral photovoltage V_{AB} on the BSCO surface and substrate as a function of laser position x. We can clearly observe that: 1) whether the laser illuminates the BSCO surface or the substrate, V_{AB} shows similar tendencies and varies almost linearly with the laser spot position when it scanned along the x-axis direction from electrodes A to B; 2) in both curves, V_{AB} is positive (negative) at a positive (negative) x and reaches its maximum value when the spot is closest to the measurement electrode. The position sensitivity, which is defined as the variation in V_{AB} brought about by a displacement of 1 mm on the x-axis at 1-mW laser power, is 20 and 16.5 μV/(mm·mW) for a laser illuminating the BSCO surface and substrate, respectively; 3) when the illumination spot is beyond the electrode, V_{AB} decays rapidly to zero.

Figure 2(a) presents the response of V_{AB} to the laser position in the y direction. V_{AB} still varies linearly with the spot position for each y, but the position sensitivity decreases with increasing absolute value of y. Moreover, the curves are roughly symmetric at $y = 0$. Adjusting the distance L of two electrodes to 3, 6, 9, 11, and 14 mm yields corresponding changes in V_{AB}, as shown in Fig. 2(b). Shorter distances between the two electrodes can clearly lead to higher sensitivity at a fixed laser position. However, if the distance between A and B is larger than 9 mm, the linearity of the curves deteriorates.

To obtain more information on LPV effects in the film, a light graphite absorption layer with a thickness of

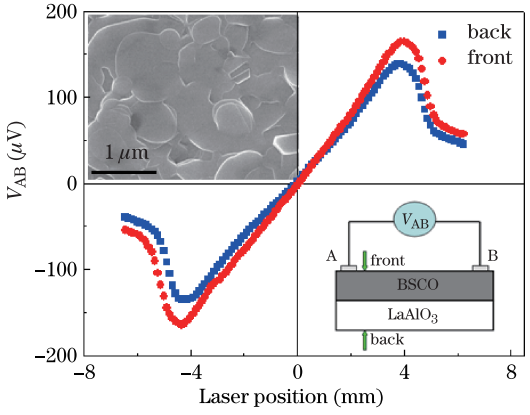

Fig. 1. (Color online) Dependence of V_{AB}on the laser spot position in the x direction with laser illumination on the BSCO surface and the substrate. The top inset shows an SEM image of the BSCO film. The bottom inset displays the schematic setup for LPV measurement.

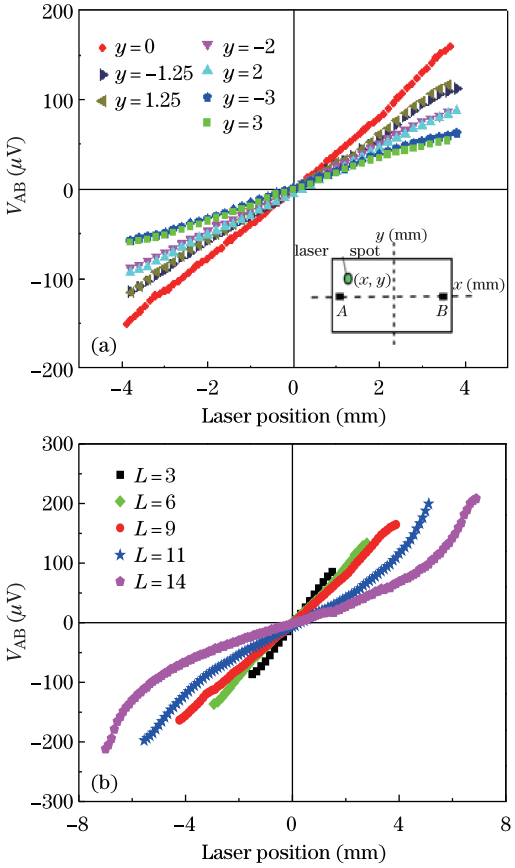

Fig. 2. (Color online) (a) Responses of V_{AB} to the laser position at different y. The inset shows a schematic diagram of the measurement plane. (b) Observed V_{AB} curves for different electrode distances (L) of 3, 6, 9, 11 and 14 mm.

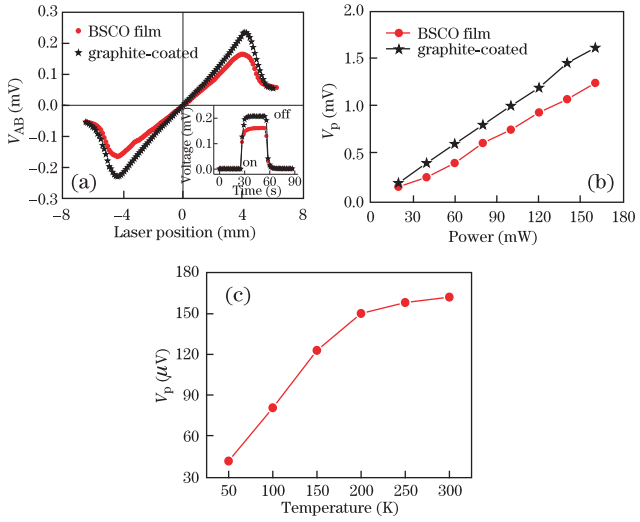

Fig. 3. (Color online) (a) Lateral photovoltage curves obtained from bare and graphite-coated BSCO films. The inset shows the time-domain profile of the voltage upon laser illumination with a spot position of $(x, y) = (4$ mm, 0mm). (b) Variations in V_p with laser power P at a fixed spot position of $(x, y) = (4$ mm, 0 mm). (c) Temperature dependence of V_p under a laser power of 20 mW.

5 μm is sprayed on the film surface to avoid the formation of photo-generated carriers brought about by direct illumination with the laser. As shown in Fig. 3(a), enhanced position sensitivity is obtained; the time-domain profile of voltage waveforms in the bare and graphite-coated films at a laser position of $(x, y) = (4,\ 0$ mm) are measured and presented in the inset of the figure. In both samples, the waveforms show identical rise and decay times, but the steady-state voltage in the graphite-coated BSCO film is 0.21 mV larger than that in the bare BSCO film (0.16 mV). Figure 3(b) shows the variation of the photovoltage amplitude (V_p) with the laser power P on the film surface when the spot position is fixed. For each power value, the V_p of the graphite-coated film appears to be larger than that of the bare BSCO film, which further demonstrates that enhanced sensitivity may be obtained from the graphite-coated film. As well, V_p increases linearly with the laser power in both samples. Finally, the temperature dependence of V_p on the bare BSCO film is measured and presented in Fig. 3(c). V_p clearly decreases with temperature, which may result from a decrease in the Seebeck coefficient of BSCO films in the plane of carrier transport at lower temperatures[12].

According to the data in Fig. 3, the conventional LPV mechanism based on photo-generated carrier effects is inapplicable for our sample. Thus, we attribute LPV effects to thermoelectric phenomena. When a film is only partially illuminated by the laser beam, a temperature gradient is formed between the illuminated and non-illuminated areas. As the carrier mobility is much higher in heated zones than in unheated ones, major carriers tend to flow from the illuminated zone to the nonilluminated region and establish a transient electric field. If the distance between the laser spot position to electrodes A and B varies, the quantity of the collected carriers on the two probe electrodes also differs, thereby generating V_{AB}. V_{AB} is also proportional to the temperature gradient between electrodes A and B because of nonuniform heating by the laser as well as the Seebeck coefficient of the material in the plane of carrier transport.

The following thermoelectric mechanism helps explain our observed results. When the laser spot is at the center of the two electrodes, V_{AB} is zero because of diffusion symmetry. If the light spot is close to one electrode, the electric potential in this electrode is lower than that in the other electrode because BSCO is a p-type material and more holes are collected at the colder electrode than at the warmer one. Since the temperature gradient along the film surface caused by laser irradiation on the substrate side is identical to that observed by laser irradiation on the film side, two V_{AB} curves in Fig. 1 exhibit similar trends with the spot position x; slightly lower values on the substrate side may be attributed to surface scattering[13]. Comparing the absorption spectra of the bare and graphite-coated BSCO films[14], the graphite layer appears to increase light absorption, which implies that higher laser powers may be effectively used to heat the film. Thus, a larger temperature gradient as well as higher V_{AB} is obtained in the graphite-coated sample. However, despite these interesting findings, other properties of the LPV effect in the film, such as the quantitative temperature distribution of the film under heated laser power and the length of the effective linear interval of the LPV signal, have yet to be satisfactorily clarified; thus, further theoretical and experimental investigations are of extreme importance in this field.

The LPV effect observed in the present BSCO film is fairly different from the laser-induced transverse voltage reported in Refs. [7,9,14] in which the origin of the transverse voltage is the anisotropic Seebeck effect. Its typical characteristic is that heat and electric energy flow through the film perpendicular to each other, and it is effective only in *c*-axis-tilted thin films or multilayers. Moreover, during the measurement, the laser spot must be located exactly at the center of the two electrodes. In the present work, LPV signals are observed in untilted BSCO films and are believed to be due to the temperature gradient and variations in carrier mobility between the two electrodes brought about by the asymmetric radiation of the laser. In other words, heat and electric energy flow through the film in the same plane.

In conclusion, the LPV effect is observed in bare and graphite-coated BSCO films. Enhanced position sensitivity observed in the graphite-coated film can be attributed to improvements in light absorption and photothermal conversion at the graphite layer. Results imply that LPV signals in the film are caused by the temperature gradient and variations in carrier mobility between illuminated and nonilluminated regions. Selection of appropriate light absorbers to increase the temperature gradient or thermoelectric materials with large Seebeck coefficients are alternative methods for improving the position sensitivity of the LPV effect. The present results provide novel insights into the design of position-sensitive photo (thermal) detectors based on thermoelectric effects.

This work was supported by the National "973" Program of China (No. 2011CB612305), the National Natural Science Foundation of China (No. 51372064), the Nature Science Foundation for Distinguished Young Scholars of Hebei Province, China (No. 2013201249), and the Science and Technology Research Projects of Colleges and Universities in Hebei Province (No. QN20131040).

References

1. H. C. Hsu, W. L. Lee, K. K. Wu, Y. K. Kuo, B. H. Chen, and F. C. Chou, J. Appl. Phys. 111, 103709 (2012).
2. G. W. Yan, L. Yu, Y. Wang, H. Zhang, P. X. Zhang, and H.-U. Habermeier, J. Appl. Phys. **110,** 103102 (2011).
3. S. Zhang, L. Chen, and S. Zhuang, Chin. Opt. Lett. **10,** 110401 (2012).
4. Z. Q. Lü, K. Zhao, H. Liu, N. Zhou, H. Zhao, L. Gao, S. Q. Zhao, and A. J. Wang, Chin. Opt. Lett. **7,** 718 (2009).
5. L. H. Yin, R. Ang, Y. N. Huang, H. B. Jiang, B. C. Zhao, X. B. Zhu, W. H. Song, and Y. P. Sun, Appl. Phys. Lett. **100,** 173503 (2012).
6. S. F. Wang, Z. L. Bai, H. F. Wang, Q. Lü, J. L. Wang, and G. S. Fu, J. Alloy. Comp. **554,** 254 (2013).
7. S. F. Wang, J. C. Cheng, X. H. Zhao, S. Q. Zhao, L. P. He, M. J. Chen, W. Yu, J. L. Wang, and G. S. Fu, Appl. Surf. Sci. **257,** 157 (2010).
8. T. Yamamoto, K. Uchinokura, and I. Tsukada, Phys. Rev. B **65,** 184434 (2002).
9. G. Y. Yan, S. F. Wang, S. S. Chen, F. Q. Liu, Z. L. Bai, J. L. Wang, W. Yu, and G. S. Fu, Appl. Phys. A **111,** 1203 (2013).
10. S. F. Wang, Z. C. Zhang, L. P. He, M. J. Chen, W. Yu, and G. S. Fu, Appl. Phys. Lett. **94,** 162108 (2009).
11. L. Du and H. Wang, Opt. Express **18,** 9113 (2010).
12. S. F. Wang, L. P. He, E. Dogheche, J. C. Chen, J. L. Wang, M. J. Chen, W. Yu, and G. S. Fu, Thin Solid Films **518,** 6829 (2010).
13. S. Q. Zhao, W. W. Liu, L. M. Yang, K. Zhao, H. Liu, N. Zhou, A. J. Wang, Y. L. Zhou, Q. L. Zhou, and Y. L. Shi, J. Phys. D: Appl. Phys. **42,** 185101(2009).
14. G. Y. Yan, H. L. Zhang, Z. L. Bai, S. F. Wang, J. L. Wang, W. Yu, and G. S. Fu, Chin. Phys. Lett. **30,** 046801 (2013).